YTUP

Journal of Thermal Engineering
https://jten.yildiz.edu.tr/
https://doi.org/10.47481/jten.0088

RESEARCH ARTICLE

Coupled effects of catalyst–ionomer ratio and hot-press load on the performance of proton exchange membrane fuel cells

Prem Kumar T.[1,*], Manoj Kumar P.[2], Biji P.[3], Vivek V. G.[4]

[1]Associate Professor, PSG Institute of Technology and Applied Research, Coimbatore, 641062, India
[2]Professor, PSG Institute of Technology and Applied Research and Coimbatore, 641062, India
[3]Professor, PSG Institute of Advance Studies and Coimbatore, 641004, India
[4]Research Scholar, PSG Institute of Technology and Applied Research and Coimbatore, 641062, India

Abstract

The use of sustainable energy is of great importance in today's world due to environmental issues and the lack of fossil fuels. Proton-exchange membrane fuel cells are a potential solution. The catalyst-to-ionomer ratio and the hot-press load are two important parameters that substantially affect the performance of the membrane electrode assembly. If the catalyst-to-ion-ion-ion-ion-ionomer ratio is too high, it can impair material bonding and cause uneven catalyst distribution; if it is too low, it can result in poor performance due to an insufficient catalyst amount. Likewise, too high a hot-press load can damage the porous catalyst layer, while too low a hot-press load increases the contact resistance between the catalyst-coated membrane and the gas diffusion layer. Optimization studies were performed on a 6.25 cm^2 proton exchange membrane fuel cell with catalyst coated membrane-membrane electrode assembly at a loading of 0.15 mgPt cm-2. The best performance was achieved at a catalyst-ionomer ratio of 3:1 and a hot-press load of 160 kg. The statistical analysis with interaction plots and derived equations confirmed the correlation between the deviation value of 710 W m^{-2} (summed individual impact and integrated effect) and the traditional interaction effect value of 355 W m-2 (ratio of 2) and confirmed by the experimental results. The typical interaction effects are theoretically straightforward, and the deviation value provided here better depicts the influence of parameter interactions and provides a more reliable tool for performance measurement. The optimized catalyst-coated membrane electrode assembly showed a 5.8% improvement compared with a commercial membrane electrode assembly, mainly due to the optimized catalyst-to-ionomer ratio and hot-press load parameters. This work improves quantification and introduces a new evaluation metric, the deviation value, which can be extended to larger proton-exchange membrane fuel cell stacks, enabling a significant advance in the fundamental understanding of membrane electrode assembly design and in its practical application to sustainable energy systems.

Keywords: Catalyst-to-ionomer ratio, deviation value, hot press load, interaction effect, maximum power density, proton exchange membrane fuel cell

Cite this article as: Prem Kumar, T., Manoj Kumar, P., Biji, P., & Vivek, V. G. (2026). Coupled effects of catalyst–ionomer ratio and hot-press load on the performance of proton exchange membrane fuel cells. Journal of Thermal Engineering, 12(6), 2132–2143. https://doi.org/10.47481/jten.0088

1. Introduction

Renewable energy is essential to reduce the dependence on fossil fuels, and hence the environmental damage can be reduced (Heidarnejad P., 2021; Solanki A., 2021). Proton exchange membrane fuel cell (PEMFC)is one of the green energy technologies that converts the chemical energy of hydrogen and oxygen directly into electrical energy (Taner., 2019). PEMFCs can effectively balance the energy demands of the future since they have high power density at low operating temperatures (Routh A et al., 2024; Ozdogan, M et al., 2019; Khelaifa, K., et al., 2024; Zhou Z Q et al., 2025). The performance of PEMFCs depends on the electrochemical reactions that take place at the membrane electrode assemblies (Jo et al., 2017; Thiyagarajan et al., 2021). Thus, the choice of materials for electrodes and electrolytes is important for efficient performance. Platinum,

*Corresponding Author
E-mail Adress: prem50567@gmail.com

Submitted: 30 June 2025; **Accepted:** 19 February 2026

This paper was recommended for publication in revised form by Editor-in-Chief Ahmet Selim Dalkılıç

which is a noble metal, is used as a catalyst in PEMFC as platinum supported on carbon (Okonkwo et al., 2021; Xie et al., 2017). The carbon support provides electrical connectivity between the metal particles and the gas diffusion layers. Platinum is particularly important because the half-cell reactions occur on the catalyst surface. The performance of PEMFCs depends on the electrochemical reactions that take place at the membrane electrode assemblies (Jo et al., 2017; Thiyagarajan et al., 2021). Thus, the choice of electrode and electrolyte materials is important for efficient performance. Platinum, which is a noble metal, is used as a catalyst in PEMFC as platinum supported on carbon (Okonkwo et al., 2021; Xie et al., 2017).

Ionomers wrap the membrane electrode assembly (MEA). The high excess ionomer increases the bulk and local resistance in the catalyst [Wang et al., 2019]. The effect of ionomer and water loading on the catalyst particles was quantified by Carcadea et al. (2019) and they found a best ionomer content that could increase the performance up to 39%. Chen et al. (2018) found that the amount of ionomer had a small effect on the electrochemical surface area and catalyst use but a large effect on the pore structure, oxygen transport and proton conductivity. The authors Shahgaldi et al. (2018) suggested that the best ionomer content would result in improved performance with a maximum power density of 1.3 Wcm-2. The performance of the catalyst layer of the PEM fuel cell was investigated by Alink et al. based on parameters such as the amount of ionomer in the material (2020) The authors conducted a detailed analysis to gain a better understanding of the effects of the parameters on the oxygen and ion transport and provided useful suggestions for optimization of the catalyst layer composition to improve the performance of the fuel cells. Huang et al. The effect of ionomer loading on the proton transport properties of the cathodic catalyst layer in PEM fuel cells was investigated in 2024. The ionomer content in the catalyst layer significantly affects PEMFC performance. The best ionomer loading was 30-40% and the catalyst to ionomer ratio was 2.5 for maximum performance operating parameters (Ishikawa et al., 2018). Many experimental studies have been performed to study the effect of the ratio of catalyst and ionomer [11, 13]. Best results were reported by Mohanta et al. (2020) at the ratio of 1.78 with variation of other operating parameters. Andersen and Grahl-Madsen (2016) studied ionomer with different percentages and found that the best was at 30% (catalyst to ionomer ratio of 3.33). The performance loss was attributed to the pore volume of the catalyst layer decreased with the increase of ionomer content (Yu et al., 2015). Xing et al. (2017) proposed best slope of ionomer which reduces mass resistance. The goal is to increase the porosity near the gas diffusion layer (GDL) and the catalyst layer. Ebenazer and Haridoss (2017) proposed the best ionomer loading of 0.04 mgcm-2 for maximum performance of their own selected PEMFCs. Mohanty et al. (2021) studied the effect of ionomer composition on the performance of PEMFCs (catalyst to ionomer ratio from 1.66 to 3.33). It proposed a volume ratio of 2, which could improve performance by about 7 percent.

Hot pressing is a prerequisite for MEA sandwich production. In this step, this method is used to compress the membrane, catalyst layer, and GDLs. The parameters of the hot-pressing process should be optimized with particular emphasis on the load (pressure) applied to the MEA active area. Sassin et al. (2016) studied in detail the effect of hot pressure on the performance of MEA and other factors. The catalyst-coated membrane (CCM) with a volume of 10 cm3 and a best hot-pressing pressure of 0.068 MPa performed best. However, the CCM performed poorly under the overpressure of 13 MPa. The best hot-pressing pressure for the best temperature and time was 5 MPa (Wang et al., 2022). They found that the titanium mesh was thinned by compression. Stahler et al. (2019) found that a hot-pressing pressure of 5 MPa yielded a CCM-MEA with better performance than an MEA prepared using a whole die slot. Moreover, Shen et al. (2018) found that a hot-pressing pressure of 0.8 MPa on a Nafion 115 membrane based on carbon paper is better than 0.4 MPa. In contrast, high pressure causes a decrease in contact resistance and an increase in performance. Sassin et al. (2017) reported the effect of compressive pressure on the performance of PEMFCs, where the best value for pressure was also proposed.

The researchers found that when the catalyst-to-ionomer ratio is too high, the ionomer is insufficient and the bonding between the components weakens. The ionomer ensures the uniform dispersion of the carbon supported platinum, which is critical for maximum performance, say Madhuranthakam et al. (2024). In contrast, performance is significantly degraded when the catalyst-to-ionomer ratio decreases because the amount of catalyst is insufficient compared to the ionomer. Thus, researchers often recommend the best ratio to keep performance. PEMFC performance is degraded when the porous structure in the catalyst layer is destroyed owing to excessive hot-press load or pressure. Conversely, extremely low hot-pressing pressure increases contact resistance between the catalyst layer and membrane, hindering best performance. Therefore, researchers recommend investigating and applying the best hot-pressing load or pressure to maximize PEMFC advantages according to requirements.

Although much work has been done on studying individually the effect of the catalyst-to-ionomer ratio and hot-pressing (Liu et al., 2023), the independent effect and combined effect analysis of selected design parameters using mathematical analysis has been minimally explored. (Thiyagarajan et al., 2022) proposed innovative mathematical model which was confirmed for operating parameters. However, no significant research has been conducted applying the derived mathematical model to experimental results for in-house MEA design properties, specifically to correlate statistical interaction effects with the mathematical deviation between the summed individual effects and the integrated effect. The innovative deviation value correlates more precisely with the impact of interactions than the conventional interaction effect.

2. Method

2.1. Preparation of MEA components

Membranes are central to the operation of PEMFCs. They isolate the electrodes from each other, prevent gas crossover, and transfer protons from the anode to the cathode. Nafion (DuPont, USA) membranes are widely used because they show high proton conductivity and durability. Nafion 117 was used in the current experiment. The preparation of MEA started with the treatment of the membranes. Treatment of the membrane was mainly done to remove the impurities present on the surface and to sulfonate it. The membrane was cut down into a 25 cm^2 cross-section and immersed in a beaker of 30% nitric acid (HNO_3) followed by deionized water, both for 1 hr. at 80 °C. After that, it was immersed in 1M sulphuric acid (H_2SO_4) for 1 hr. at 80 °C and finally kept in a beaker of deionized water for 1 hr. at 80 °C. Then, the proton-exchange membrane was stored in deionized water until it was ready for use. (Figure 1).

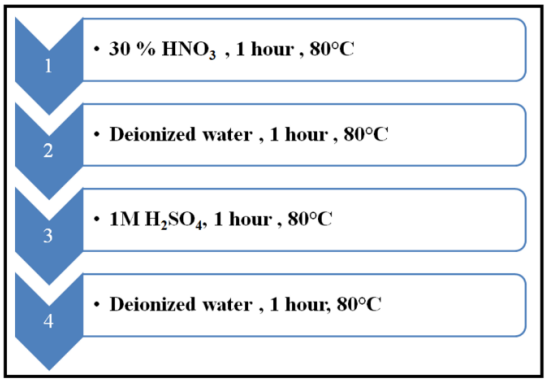

Figure 1. Flow Chart representation of treatment of membranes

The gas diffusion layer was prepared using carbon cloth cut to the size of the active area. A GDL of 6.25 cm^2 had been cut, and it was hydrophobized with the help of polytetrafluoroethylene (PTFE) of concentration (Figure 2). The GDL was kept at 15% PTFE for 2 minutes and then kept in the hot air oven at 100 °C for 1 hour. It was then placed in the open air and dried for 10 hours, until it reached room temperature.

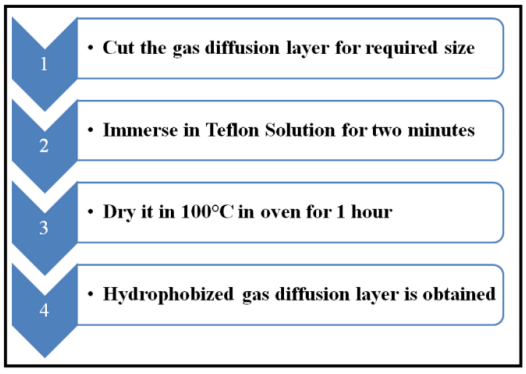

Figure 2. Flow chart representation of hydrophilization of GDL

The catalyst ink was prepared using 51.6 mg of Pt/C (platinum-supported carbon) powder, 1115 mg of ultrapure water, 945 mg of IPA (isopropyl alcohol), and 169 mg of ionomer (Nafion) solution at 15% concentration. 40% Pt/C powder was measured into a Petri dish; ultrapure water was then added, and the dish was gently shaken to ensure that the Pt/C powder was fully wet, preventing sparking or ignition upon contact with IPA in the next step. Then, IPA was added dropwise to the wet Pt/C. Then, the Nafion solution (ionomer) was added to the Petri dish having the above mixture. Then, an IPA solution of 1027 mg was added again. Then, the ink was kept in a small beaker with the cap completely closed and stirred at low rpm for 12 hours to ensure complete mixing of the ingredients. The catalyst-to-ionomer ratios considered were 3:1 and 1.5:1, achieved by varying the ionomer mass while keeping the catalyst quantity constant. The steps followed in catalyst ink preparation are shown in Figure 3.

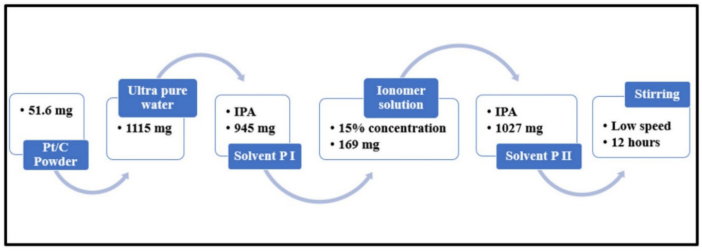

Figure 3. Procedure for preparation of catalyst ink

2.2. Catalyst-coated membrane (CCM) and catalyst-coated substrate (CCS)

In CCM-MEA, the treated membrane was placed on a hot perforated vacuum plate, which was kept at 80 °C. It was covered with a transparent heat-resistant mask sheet that had been cut according to an active area of 2.5 cm x 2.5 cm (6.25 cm^2) at the center. A vacuum pump was used to remove the air gap between the hot plate and the treated membrane. Catalyst ink was sprayed through a nozzle at 1 bar gauged pressure onto the anode side and allowed to cool on the hot plate for 5 to 10 minutes. Then the membrane was inverted, and the same process was repeated on the cathode side, as shown in Figure 4. The components were arranged so that the anode GDL adhered to the anode side and the cathode GDL adhered to the cathode side of the catalyst-sprayed part in the CCM. It was placed on the cohesive non-stick sheet and kept within the plates. The plates were heated to 120°C and the entire setup was pressed using a hydraulic press with the selected load (160 kg or 460 kg based on the experiments) for 2 minutes. As the load was retracted, the components that were sandwiched were taken out. The catalyst-coated membrane and the GDL hot-pressed CCM-MEA are shown in Figure 5.

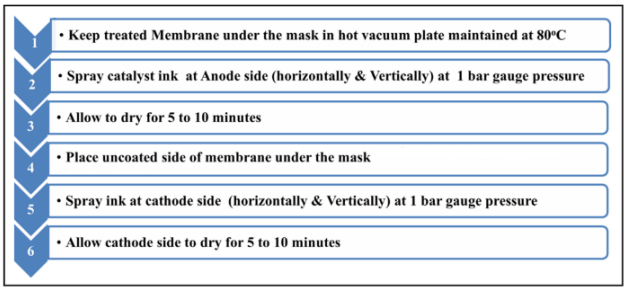

Figure 4. Membrane catalyst coating procedure

In CCS, it was fabricated from three components: an anode gas diffusion electrode (GDE), a cathode GDE, and a treated membrane. All three components were assembled so that the anode GDE and cathode GDE adhered precisely to the center of the membrane on each side. It was enclosed in a Kapton sheet and placed in the hot press. Within the hydraulic hot press, the plates were heated to 120 °C and a load (160 kg and 460 kg) was applied. After the load was withdrawn and the components removed, the pressed membrane was designated GDE-MEA.

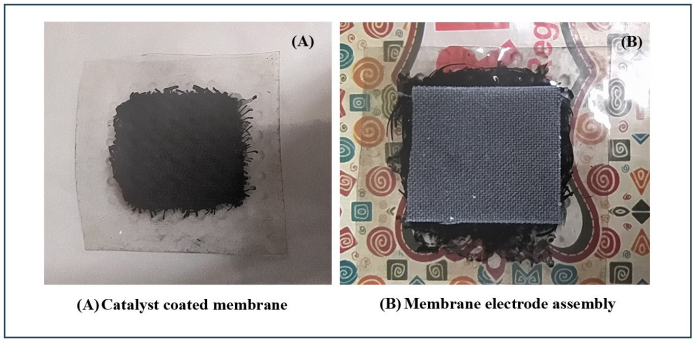

Figure 5. CCM (Catalyst-coated membrane) and membrane electrode assembly

2.3. Assembling and testing methodology

The performance of a single-cell PEMFC was evaluated in the fuel cell test station Biologic FCT 50 [250 W capacity with inbuilt voltmeter (5 V max, +/- 0.004 V uncertainty), ammeter (50 A max, +/- 0.014 A uncertainty), calculated power density (+/- 0.022 W m^{-2} uncertainty for given active area size), pressure gauges, line heaters (2 numbers), cell heater (1 number), humidifier heaters (2 numbers), humidifiers (automatic filling /dew point humidity), flow controller (hydrogen 0 - 40 liter hr^{-1}, oxygen flow rate 0 - 100 liters hr^{-1} ,+/- 0.212 mL min^{-1} uncertainty), thermocouples (+/- 0.114 °C uncertainty), and control software (FC lab)]. The experiments were also repeated with the maximum variation of 1.28%. The cell was fabricated using MEAs (CCM-MEA and CCS-MEA), carbon cloth gas diffusion layers, single-channel graphite plates, and gold-coated copper current collectors. The entire cell was held between two stainless-steel-end plates (Figure 6).

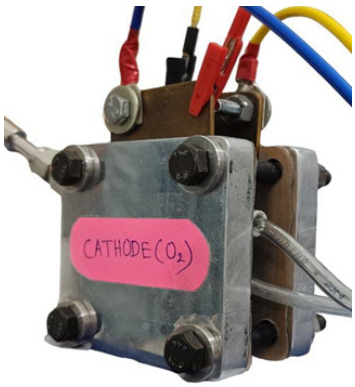

Figure 6. Assembled PEMFC

The circuit diagram of the fuel test station was shown on Figure 7. Input connections from the oxygen and hydrogen gas tanks were routed separately to the fuel cell test station mass flow meter via pressure switches and solenoid valves. The nitrogen gas line was used for purging. Solenoid valves were used to change the flow direction. The humidifiers were supplied with a water tank and a pump to pressurize the water.

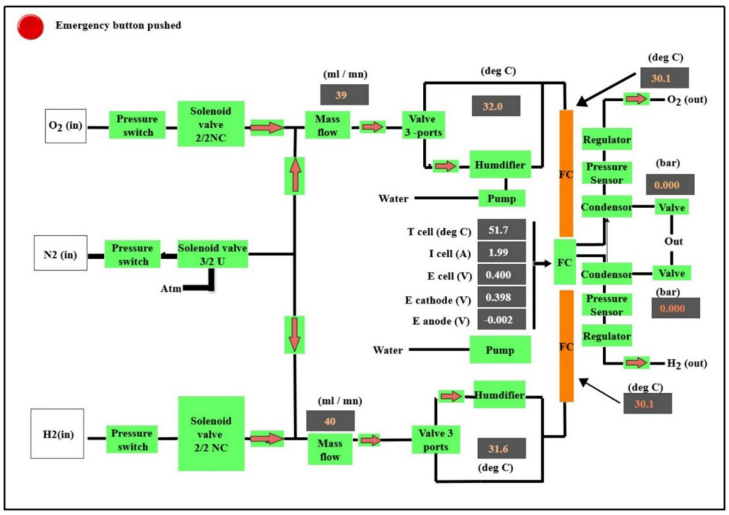

Figure 7. Circuit diagram of fuel cell test station

The humidifier's water temperature was also checked independently. Then, the main gas line was delivered to the fuel cell through a line heater. The line heater was regulated according to input temperature, which is the intake gas temperature. The complete test station was linked to the system using software, and all the input and output data could be viewed through it. The fuel cell was tested under various operating parameters. The catalyst-to-ionomer ratios considered were 3:1 and 1.5:1, achieved by varying the ionomer mass while keeping the catalyst quantity constant. The steps followed for the catalyst ink preparation are shown in Figure 3.

2.4. Design parameters

The catalyst-to-ionomer ratio varied by changing the mass of the ionomer solution (Nafion) while keeping the catalyst quantity constant (Pt/C powder). The quantities considered for the specified ratios are presented in Table 1. The levels beyond the chosen ones were found to be less efficient or did not reverse the trend. To vary the applied load on the MEA, the hot press load was adjusted using the press setup on the dial controls. Apart from the design parameters mentioned in Table 1, other parameters like platinum loading per active area (0.15 mg_{pt} per active area), temperature set point (120 °C) and time limit (2 min) for hot press, concentration of acids, time limit and temperature limit of membrane treatment, concentration of GDL hydrophilization (Teflon) coating and its drying temperature along with time were kept constant so that the parameters could be studied effectively.

Table 1. Catalyst-to-ionomer ratio and hot press load conditions

Sl. No.	Factor name	Lower level	Higher level
1	Catalyst-to-ionomer ratio	1.5:1	3:1
2	Hot press loading on MEA	Kg	kg

2.5. Statistical analysis

As the study involved two parameters, each with two levels, a conventional interaction plot was employed for the analysis. Interaction effects between hot-press load and catalyst-to-ionomer ratio were further evaluated to assess their average influence. The study investigated the average combined influence of parameters and examined the relationship between their integrated effect and the cumulative contribution of their individual effects with the help of equations 1 to 8 (Thiyagarajan et al., 2022). Interaction effect was the conventional statistical term used to determine the difference between averaged maximum power density when the combination was high and low [1-3]. It considered all possible combinations of non-analyzed parameters and therefore produced mean values. Equation 4 describes the integrated effect when the combination varies as a group from low to high levels. Equation 5 describes the summed individual impact, which accounts for individual variation in levels, using the group's high levels as the reference. The deviation value, as described in equation 7, shows the difference between the sum of individual impacts and the integrated effect, and its percentage variation with respect to the upper limit value as in equation 6. The mathematical expansion of the deviation value is shown in equation 7, which is equivalent to equation 1 multiplied by 2. Equation 8 was derived mathematically and confirmed against the experimental results for the MEA design parameters in this research. The equations and correlations were illustrated in Figures 12 and 13 to prove their application to MEA design parameters, easing understanding and further analysis.

The interaction plot was used in the study to calculate the correlation between the conventional interaction effect and the novel deviation value.

$$\text{Effect}_{\text{interact}} = \{[P_{max_{avg}}]_{\text{high}}\}_{\text{interact}} - \{[P_{max_{avg}}]_{\text{low}}\}_{\text{interact}} \quad (1)$$

$$\{[P_{max_{avg}}]_{\text{high}}\}_{\text{interact}} = \frac{\{[P_{max_{avg}}]_{\text{high}}\}_{A\&B} + \{[P_{max_{avg}}]_{\text{low}}\}_{A\&B}}{2} \quad (2)$$

$$\{[P_{max_{avg}}]_{\text{low}}\}_{\text{interact}} = \frac{\{[P_{max_{avg}}]_{\text{high \& low}}\}_{A\&B} + \{[P_{max_{avg}}]_{\text{low \& high}}\}_{A\&B}}{2} \quad (3)$$

$$\Delta[P_{max_{avg}}]_{\text{Integrated effect}} = \{[P_{max_{avg}}]_{\text{high}}\}_{A\&B} - \{[P_{max_{avg}}]_{\text{low}}\}_{A\&B} \quad (4)$$

Summed individual impact with respect to maximum limit is given as:

$$\sum\{\Delta[P_{max_{avg}}]_{\text{Individual impact}}\} = [\{[P_{max_{avg}}]_{\text{high}}\}_{A\&B} - \{[P_{max_{avg}}]_{\text{high \& low}}\}_{A\&B}] + [\{[P_{max_{avg}}]_{\text{high}}\}_{A\&B} - \{[P_{max_{avg}}]_{\text{low \& high}}\}_{A\&B}] \quad (5)$$

$$\text{Upper limit Percentage deviation} = \frac{\sum\{\Delta[P_{max_{avg}}]_{\text{Individual impact}}\} - \Delta[P_{max_{avg}}]_{\text{Integrated effect}}}{[P_{max}]_{\text{upper limit i.e. experiment 1}}} \times 100 \quad (6)$$

$$\text{Deviation value in terms of power density at} \frac{W}{m^2} = \sum\{\Delta[P_{max_{avg}}]_{\text{Individual impact}}\} - \Delta[P_{max_{avg}}]_{\text{Integrated effect}} = \{[P_{max_{avg}}]_{\text{high}}\}_{A\&B} + \{[P_{max_{avg}}]_{\text{low}}\}_{A\&B} - \{\{[P_{max_{avg}}]_{\text{high \& low}}\}_{A\&B} + \{[P_{max_{avg}}]_{\text{low \& high}}\}_{A\&B}\} \quad (7)$$

$$\text{Deviation value in terms of power density at} \frac{W}{m^2} = 2 \times \text{Effect}_{\text{interact}} \quad (8)$$

3. Result and discussion

3.1. Effect of catalyst-to-ionomer ratio

As discussed previously, the maximum power density for different CIRs is shown in Table 2. The MEA constructed at the specified ratio was evaluated in a fuel-cell test station, as described previously, under constant hydrogen and oxygen flow rates to decide its performance.

From Table 2, the highest power density was achieved at 0.46 V and 0.4 V with the values of 2,820 W m^{-2} and 1,540 W m^{-2} for experiments 1 and 2, respectively. Table 2 shows that decreasing the catalyst-ionomer ratio from 3:1 to 1.5:1 under a hot-press load of 160 kg resulted in a 45.39% drop in performance compared with the upper-limit power density achieved in experiment 1. Figure 8 depicts the VI and power density-current density of both trials.

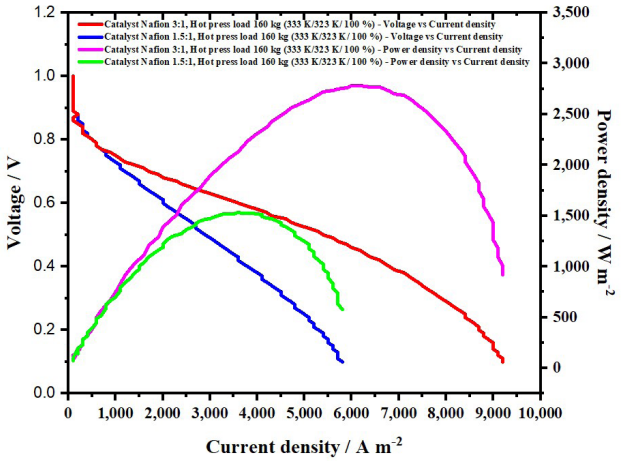

Figure 8. Effect of catalyst to ionomer ratio

The activation, ohmic-loss, and concentration zones could be seen on the VI curve. From the VI curves of both experiments, it was inferred that the voltage drop in the activation loss zone was relatively smaller than that in CIR 1.5:1, which resulted in an increase in the maximum power density in the former experiment. The above results were in line with the experimental study of research (Alink et al., 2020), where a higher CIR reduces voltage drop in the activation region because more catalyst surface becomes available for oxidation-reduction reaction and ionomer-induced site blocking is minimized, thereby lowering the kinetic barrier.

The voltage drop in the ohmic loss zone for CIR 1.5:1 was steeper than that for CIR 3:1. The percentage of catalyst, relative to the amount of ionomer, was higher in CIR 3:1. A high ionomer percentage could improve proton transfer, but a reduced catalyst percentage might decrease performance because of slower reaction kinetics. A high percentage of ionomer could also lead to an increase in contact resistance. These were the possible reasons for the drop in performance at CIR 1.5:1.

Table 2. Effect of catalyst-to-ionomer ratio

Sl. No.	Exp. No.	Catalyst-to-ionomer ratio	Hot press load / kg	Maximum power density / W m^{-2}
1	1	3:1	160	2,820
2	2	1.5:1	160	1,540
Percentage reduction in power density with respect to the upper limit, i.e., experiment 1				45.39%

3.2. Effect of hot press load on MEA

The maximum power density for different hot-press loads of the same CIR is shown in Table 3. From Table 3 it was clear that the maximum power density was obtained at 0.42 V, which was equal to 2,190 W m^{-2} for the best operating parameters combination for experiment 3. It could be inferred that increasing the hot-press load from 160 kg to 460 kg, with the base CIR 3:1, reduced performance by 22.34% compared to the upper limit (i.e., experiment 1). The results proved the impact of high hot press load, which can collapse pore networks and restrict gas diffusion (Zhao et al., 2023). The VI and power density-current density of both experiments were shown in Figure 9

Table 3. Effect of hot press load on MEA

Sl. No.	Exp. No.	Catalyst-to-ionomer ratio	Hot press load / kg	Maximum power density / W m^{-2}
1	1	3:1	160	2,820
2	3	3:1	460	2,190
Percentage reduction in power density				22.34%

Figure 9 shows that the activation-zone voltage drop in experiment 3 was marginally higher than in experiment 1. The voltage drop in the ohmic loss zone was steeper in the hot-press experiment with a 460 kg load than in the hot-press experiment with a 160 kg load. The increased hot press loads improved contact between the GDL and the catalyst. A decrease in contact resistance could be achieved, but the GDL could be damaged, resulting in reduced reaction kinetics. The results of the trials showed that the impact of the latter outweighed the advantages of the former, which could be a probable cause of the 22.34% performance reduction in experiment 3 relative to experiment 1.

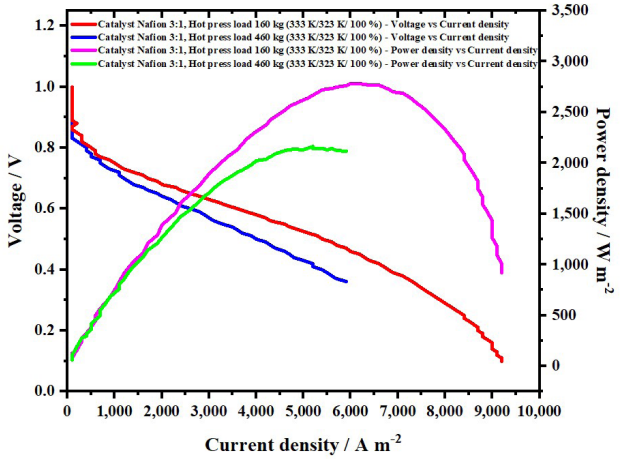

Figure 9. Effect of catalyst-ionomer ratio and hot press load on MEA

3.3. Effect of combination of parameters

In this analysis, both CIR and hot-press load were varied compared to those in the base reference experiment 1 to investigate their combined influence. In experiment 4, the hot press load increased to 460 kg and the CIR reduced to 1.5:1; the results were compared with those of experiment 1 to decide the combined impact. From Table 4, the peak power density was obtained as 1,620 W m^{-2} at 0.42 V.

As previously noted, the increase in hot-press load from 160 kg to 460 kg and the reduction in CIR from 3:1 to 1.5:1 resulted in decreased maximum power density compared with the prior configuration. Nevertheless, in experiment 4, the predicted percentage decrease was 67.73%, but the actual reduction was 42.55%, a difference of 25.17% from the predicted decrease, showing that interactions had an effect. Figure 10 depicts the VI, power density, and current density of each trial. All four tests are shown on Figure 11.

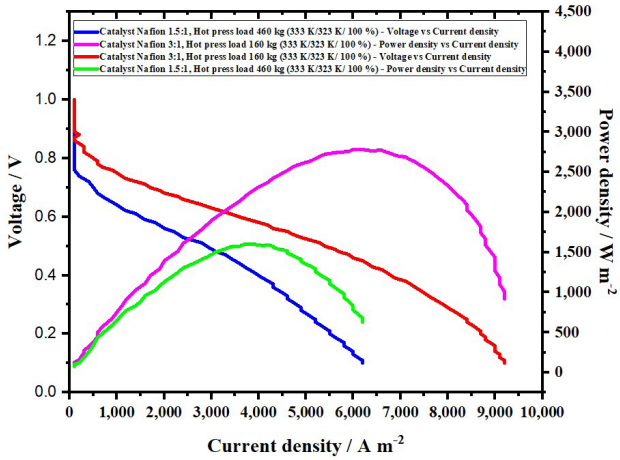

Figure 10. Effect of catalyst ratio and hot press load on MEA

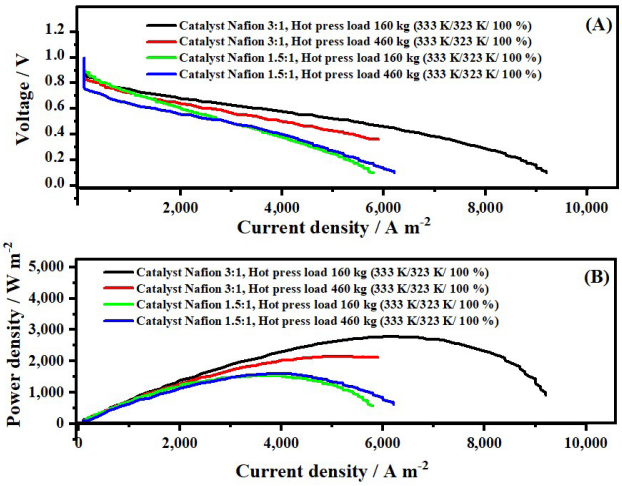

Figure 11. Effect of combination of parameters

Activation, ohmic-loss, and concentration zones could be found in VI curves. Figure 10 and Figure 11 show that the voltage drop in the activation-loss zone of experiment 4 was substantially greater than in the other experiments. In experiments 3 and 4, the MEAs were hot compressed under the same load of 460 kg. Higher voltage drops in experiment 4 (due to lower CIR) compared with experiment 3 were likely one of the causes of the percentage difference between the integrated effect and the summation of individual effects. Results proved that the ohmic losses were large for CIR 1.5:1 under a base hot-press load of 160 kg, compared with the same CIR under a base hot-press load of 460 kg. It could be deduced that lower CIR with a high hot press load could increase performance in the ohmic zone, but the same could lead to higher losses in the activation zone. However, the advantages of the former outweighed the impacts of the latter; so, the performance decline in experiment 4 was smaller than the summed individual impacts of experiments 2 and 3, a finding that will be explored in detail in the statistical analysis.

Table 4. Effect of combination of parameters

Sl. No.	Exp. No.	Catalyst-to-ionomer ratio	Hot press load / kg	Maximum power density / W m^{-2}	Percentage deviation in power density with respect to reference / %
1	1	3:1	160	2,820	-
2	2	1.5:1	160	1,540	-45.39
3	3	3:1	460	2,190	-22.34
4	4	1.5:1	460	1,620	-42.55
Expected summation effects					-67.73
Deviation value in terms of percentage					-25.17
Deviation value in terms of peak power density					-710 Wm^{-2}

3.4. Statistical results

3.4.1. Main effect

As two parameters had been selected, the total options as per 2^n correlation were four, as displayed in Table 5. The main effect shows the deviation in maximum power density during level changes from low to high, as given in Table 6. The main effect was greater for the catalyst-to-ionomer ratio and smaller for the hot press load, with percentage deviations of 32.80% and -9.75%, respectively.

Table 5. Factors along with levels

Sl. No.	Factor	Symbol	Low-level (-1)	High-level (+1)	Factor abbreviation
1	Catalyst-to-ionomer ratio	A	1.5:1	3:1	CIR
2	Hot press loading	B	160 kg	460 kg	HPL

Table 6. Main effects and percentage deviation for parameters

Description	A	B
Mean values of maximum power densities for the upper level in W m^{-2}	2,505	1,905
Mean values of maximum power densities for the lower level in W m^{-2}	1,580	2,180
Main effect / W m^{-2}	925	-275
Decrease in terms of percentage	32.80	-9.75

3.4.2. Interaction effect

Only one conceivable combination of the stated parameters (AxB) was achievable in this investigation. Table 7 presents individual parameter levels, combination levels, and experimental maximum power density. Table 8 shows the interaction effect and the percentage deviation for AxB. Figure 12 illustrates the interaction effects among the selected parameters. As shown in equations 1 to 3, the average of A1 and B2 indicated the average maximum value of power density when the combination was at a high level. The average of A2 and B1 indicated the value corresponding to a low level of combination. The difference between the above values explains the interaction effect. The reference was taken when both CIR and HPL were at a high level, i.e., B2. The interaction effect was 355 W m^{-2} considering the difference between high levels of interaction averaging 1,865 W m^{-2} and the contradictory level of 2,220 W m^{-2}.

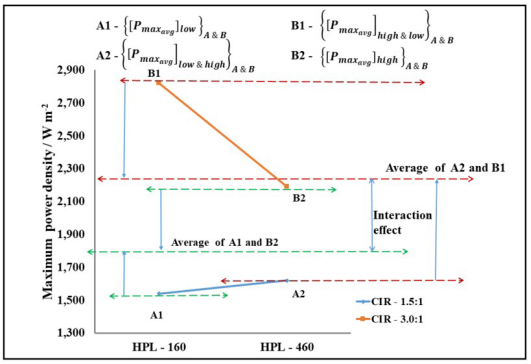

Figure 12. Interaction effect of parameters

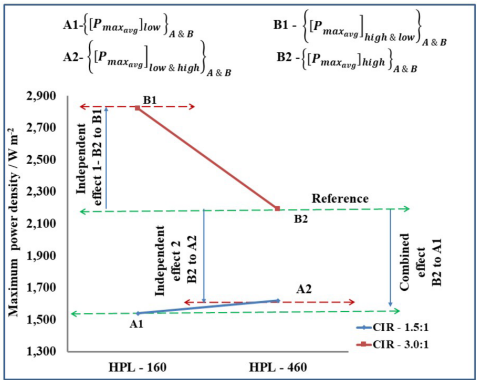

Figure 13. Summed individual impact and integrated effect

Figure 13 illustrates the summed individual impact values and integrated effect values (equations 4 and 5). Point B2 was shown as a reference where levels of both parameters were high. Individual impact was studied as shown in the figures (i.e., B2 to A1 and B2 to A2), where CIR and HPL were varied individually from their higher to their lower levels. The summation of the above effects shows the total individual effect. The second study involved a variation from B2 to A1 in which levels of both CIR and HPL varied simultaneously; this was referred to as the integrated or combined effect. The deviation between the two parameters was termed the deviation value, as showed in Equation 7. Data from the table (Table 9) showed that the difference between summed individual effects and the integrated effect was 710 W m^{-2}, or 25.17%.

As shown in figures (Figure 12 & Figure 13) for CIR 3:1, increasing the hot press load from 160 kg to 460 kg resulted in a higher fall in performance, resulting in an average loss of 2.1 W m^{-2} per kg of hot press load. In comparison, increasing the hot press load from 160 kg to 460 kg for CIR 1.5:1 increased performance at a lower increment rate of 0.26 W m^{-2} per kg of hot press load. A reversal in direction and a decline in rate could have caused the divergence of the combined impact from the projected total of distinct impacts. Then, the two results, the conventional interaction effect and the deviation value— were compared to confirm Equation 8. It was seen that the deviation value (710 W m^{-2}) was two times the conventional interaction effect (355 W m^{-2}). The validation showed that the deviation value can be readily obtained from the conventional interaction effect using Equation 8.

Although the conventional interaction effect was simple to use and proportional, it could not provide the exact impact of the interaction. As shown in Figure 12 (equations 1, 2 & 3), the interaction effect compares only the combinations of levels. Low levels of the two individual parameters (equation 2) can also result in a high combined level. Hence, the interaction effect can provide a proportional comparison of the impact of interactions, but not an exact measure. The coined 'deviation value' term (as shown in Figure 13 and equation 7) shows the difference between the summed individual impacts (or independent effects) in equation 4 and the integrated effect (or combined effect) in equation 5. Here, instead of considering the levels of combinations, the level of each individual parameter is considered. This can provide a precise estimate of interaction effects, and the coined deviation value term can substantiate the conventional interaction effect term, yielding a more correct assessment of interactions.

Table 7. Impact of interactions on maximum power density

Exp. order	A (CIR)	B (HPL)/ Kg	Level A	Level B	Level A x B	Maximum power density / W m^{-2}
1	3:1	160	+1	-1	-1	2,820
2	1.5:1	160	-1	-1	+1	1,540
3	3:1	460	+1	+1	+1	2,190
4	1.5:1	460	-1	1	-1	1,620

Table 8. Interaction effect

Description	A x B
Mean values of maximum power densities for upper levels in W m^{-2}	1,865
Mean values of maximum power densities for lower levels in W m^{-2}	2,220
Interaction effect in W m^{-2}	-355

Table 9. Deviation between summed individual impact and integrated effect

Sl. No.	Description	A x B
1	Mean values of maximum power densities [both factors at a high level] [Reference] in W m^{-2}	2,190
2	Mean values of maximum power densities [high and low level] in W m^{-2}	2,820
3	Mean values of maximum power densities [low and high level] in W m^{-2}	1,620
4	Mean values of maximum power densities [both factors at a low level] in W m^{-2}	1,540
5	Summed individual impact in W m^{-2} [Equation 5]	-60
6	Integrated effect value in W m^{-2} [Equation 4]	+650
7	Deviation between summed individual impact and integrated effect [Equation 7] in W m^{-2}	-710
8	Deviation value in terms of percentage [Equation 8]	-25.17

3.4.5. Comparison of optimized MEA with commercial MEA

The performance of the fabricated, optimized MEA (experiment 1) was compared with that of a commercial MEA of the same size. All components except MEA were kept constant in both experiments. The fuel cell with commercial MEA was tested under the best combination of operating parameters and compared with the fabricated, optimized MEA (experiment 1), as shown in Table 10 and Figure 14. Although the operating temperature and inlet reactant gas temperature differed between the two MEAs (lab-made and commercial), the comparison stays valid because it focused on evaluating the peak power density under the best conditions for each MEA.

Figure 14 and Table 10 show that the laboratory-made MEA fuel cell outperformed the commercial MEA fuel cell. At 323 K operating temperature, 343 K input reactant gas inline temperature, and 100% relative humidity (RH), the highest power density of commercial MEA was 2656 W m^{-2} at 0.42 V. After testing and studies, the achieved operating parameter combination was best for both commercial and lab-made MEAs. The highest performance of the laboratory-made MEA was seen at an operating temperature of 333 K, an inline temperature of 323 K for the incoming reactant gas, and a relative humidity of 100%. A maximum power density of 2820 Watts/m2 was achieved by the combination at 0.46 volt, being a 5.82% increase over the commercial MEA.

The performance of the laboratory-made MEA was better than that of the commercial MEA, although the laboratory-made MEA had a lower platinum loading (0.15 mgpt cm-2 of active area) than the commercial MEA (0.3 mgpt cm-2 of active area). This was attributed to the best catalyst-to-ionomer ratio and hot-press loading. The VI-curve indicated that the activation loss of the commercial MEA was slightly higher than that of the optimized lab-made MEA. The slope of the voltage drop in the ohmic-loss region was higher in the commercial MEA than in the lab-made MEA.

The commercial MEA has a higher platinum loading, resulting in a lower concentration loss than the laboratory MEA. This study was carried out by Schneider et al. in 2023. The surface transport resistance and concentration polarization resistance of the catalyst decrease with increasing current density. This is due to the increasing current density. A larger catalytic surface area reduces the local current density per unit platinum surface area and consequently leads to oxygen depletion at the active sites. Because the highest power density point is obtained in the ohmic zone, the performance drop in the concentration zone of the lab-made MEA would not be substantial in real-world applications. The commercial MEA was GDL coated, while the lab-made MEA was CCM type, which could have also contributed to the superior performance of the latter.

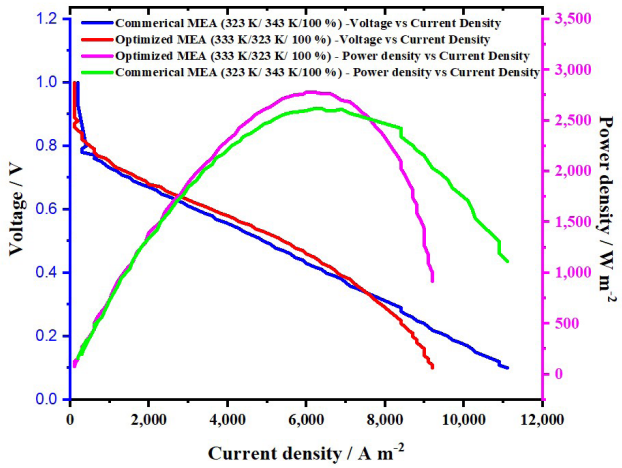

Figure 14. Comparison of optimized MEA with commercial MEA

Table 10. Comparison of optimized MEA with commercial MEA

SI No	Exp. No.	Procurement	Coating type	Maximum power density / W m^{-2}
1	1	Lab-made	GDL coated	2,820
2	7	Commercial	CCM	2,656
Percentage increment with respect to experiment 1				5.82%

4. Conclusion

The performance of single-cell proton exchange membrane fuel cells with lab-made catalyst-coated membranes and membrane electrode assemblies, in terms of the voltage–current curve and maximum power density, was studied in detail for different design parameters, such as catalyst-to-ionomer ratio and hot-press load at different levels, which have been chosen based on literature review and trial and error. The better performance was obtained with the highest power density of 2,820 W m^{-2} with a catalyst-to-ionomer ratio of 3:1 and a hot press load of 160 kg. Statistical analysis was used to calculate the mean value while taking into account all possible non-analyzed parameters. The main effect of catalyst-to-ionomer ratio was obtained as 925 W m^{-2}, whereas for hot press load the value was 275 W m^{-2}. The conventional interaction effect for the lonely combination was 355 W m^{-2} which is equal to 25.17% with respect to the upper limit. The mathematical deviation value between the summed individual impact and the integrated effect was found to be 710 W m^{-2}. The obtained value supported a novel correlation between the deviation value and the conventional interaction effect, with the former being twice the latter. Hence, the correlation can be used to obtain a statistically more precise estimate of deviation than the mathematically simple interaction effect, whereas the latter gives a clearer picture of the effect of interactions. The optimized lab-made proton exchange membrane fuel cell with a catalyst-coated membrane–electrode assembly was compared with a commercially available similar-sized membrane electrode assembly and a difference of 5.82% was found, mainly due to the optimized catalyst-to-ionomer ratio and hot press load. The study can be further extended to include various design parameters of the membrane electrode assembly, enabling a more comprehensive statistical analysis. Additionally, it can be applied to proton exchange membrane fuel cell stacks in optimization studies. The proposed innovative equation may also be validated on larger proton exchange membrane fuel cell stacks, making it more relevant to practical applications and providing a clearer representation of the combined effects of multiple design parameters.

Acknowledgement

This work was supported by DST-HFC (Ref: DST/TMD/HFC/2K18/55(C)/1) for financial support and by PSG Institutions, Coimbatore, for providing the necessary facilities and other support to carry out this work.

Author contributions statement

Prem Kumar Thiyagarajan: Conceptualization, method, investigation, experimental work, data curation, formal analysis, software, visualization, validation, writing – original draft preparation. Manoj Kumar P: Conceptualization, supervision, method, project administration. Biji P: Formal analysis, validation, data interpretation. Vivek V G: Analysis, Writing – review & editing.

Declaration of interests

The authors declare that they have no competing interests.

Data availability statement

The data supporting the findings of this study are available from the corresponding author upon reasonable request.

Declaration of generative AI and AI-assisted technologies in the writing process

The authors used Quillbot, an AI enabled language editing tool by OpenAI, to enhance grammar, sentence structure and readability of this manuscript. The AI tool was not used to generate scientific results, analyze data, interpret findings or draw conclusions. The authors took full responsibility for the final manuscript, including all scientific content, analyses, interpretations, and conclusions, which they developed, verified, and approved.

Nomenclature

$Effect_{interact}$	Integration effect in W m^{-2}
$\{[P_{max_{avg}}]_{high}\}_{interact}$	Mean of highest power density during high interaction in W m^{-2}
$\{[P_{max_{avg}}]_{low}\}_{interact}$	Mean of highest power density when interaction is low in W m^{-2}
$\Delta [P_{max_{avg}}]_{Integrated\ effect}$	Integrated effect in W m^{-2}
$\sum \{\Delta [P_{max_{avg}}]_{Individual\ effects}\}$	Sumed Individual effects in W m^{-2}
$\{[P_{max_{avg}}]_{high}\}_{A\&B}$	Mean of highest power density when both parameters' level is at high in W m^{-2}
$\{[P_{max_{avg}}]_{low}\}_{A\&B}$	Mean of highest power density when both parameters' level is at low in W m^{-2}
$\{[P_{max_{avg}}]_{high\ \&\ low}\}_{A\&B}$	Mean of highest power density when parameters' level is at high and low in W m^{-2}
$\{[P_{max_{avg}}]_{low\ \&\ high}\}_{A\&B}$	Mean of highest power density when parameters' level is at low and high in W m^{-2}
$[P_{max}]_{upper\ limit}$	Highest power density of upper limit which is considered as reference in W m^{-2}

Abbrevations

CCM	Catalyst-coated Membrane
CCS	Catalyst-coated Substrate
CIR	Catalyst- Ionomer Ratio
GDE	Gas Diffusion Electrode
GDL	Gas Diffusion Layer
HPL	Hot Press Load
IPA	Iso Propyl Alcohol
MEA	Membrane Electrode Assembly
ORR	Oxygen Reduction Reaction
PEMFC	Proton Exchange Membrane Fuel Cell
Pt/C	Platinum supported Carbon

PTFE	Polytetrafluoroethylene
RH	Relative Humidity
VI	Voltage Current

References

[1] Alink, R., Singh, R., Schneider, P., Christmann, K., Schall, J., Keding, R., & Zamel, N. (2020). Full parametric study of the influence of ionomer content, catalyst loading and catalyst type on oxygen and ion transport in PEM fuel cell catalyst layers. Molecules, 25(7), 1523. https://doi.org/10.3390/molecules25071523

[2] Andersen, S. M., & Grahl-Madsen, L. (2016)). Interface contribution to the electrode performance of proton exchange membrane fuel cells – Impact of the ionomer. International Journal of Hydrogen Energy, 41(3), 1892–1901. https://doi.org/10.1016/j.ijhydene.2015.10.04.

[3] Carcadea, E., et al. (2019). Influence of catalyst structure on PEM fuel cell performance – A numerical investigation. International Journal of Hydrogen Energy, 44(25), 12829–12841. https://doi.org/10.1016/j.ijhydene.2018.12.155.

[4] Chen, Y., Zhong, Q., Li, G., & Pan, M. (2018). Electrochemical study of temperature and Nafion effects on interface property for oxygen reduction reaction. Ionics, 24(12),3905–3914. https://doi.org/10.1007/s11581-018-2533-3

[5] Ebenezer, D., & Haridoss, P. (2017). Effect of crosslinked poly(vinyl alcohol)/sulfosuccinic acid ionomer loading on PEMFC electrode performance. International Journal of Hydrogen Energy, 42(7),4302–4310. https://doi.org/10.1016/j.ijhydene.2017.01.124

[6] Heidarnejad, P., & Noorpoor, A. (2021). Performance comparison and investigation of two different renewable energy fueled multigeneration systems. Journal of Thermal Engineering, 7, 1039–1055. https://doi.org/10.18186/thermal.977707

[7] Huang, Y., Theodorakis, P. E., Zeng, Z., Wang, T., & Che, Z. (2024). Ionomer structure and component transport in the cathode catalyst layer of PEM fuel cells: A molecular dynamics study. Journal of Chemical Physics, 160(4), 044910. https://doi.org/10.1063/5.0184566

[8] Ishikawa, H., Yogo, K., Kawamata, H., & Matsumoto, K. (2018) Effects of Pt and ionomer ratios on the structure of catalyst layer: A theoretical model for polymer electrolyte fuel cells. Journal of Power Sources, 374, 196–204. https://doi.org/10.1016/j.jpowsour.2017.11.026

[9] Jo, A., Song, C., Lee, J., Park, Y., & Kim, S.(2017). Modeling and analysis of a 5 kWe HT-PEMFC system for residential heat and power generation. International Journal of Hydrogen Energy, 42(3), 1698–1714. https://doi.org/10.1016/j.ijhydene.2016.10.152

[10] Routh, A., Ghosh, S., Dey, I., Rahaman, M., & Ghosh, A. (2024). Optimization of PEMFC pressure control using fractional PI/D controller with non-integer order: Design and experimental evaluation. Engineering Research Express, 6(2), 025001. https://doi.org/10.1088/2631-8695/ad33ff

[11] Khelaifa, K., Atia, A., Moussa, H. B., & Naroura, A. (2024). Critical investigation of microchannel design effect on thermal performances of a PEM fuel cell. Journal of Thermal Engineering, 10(1), 36–49. https://doi.org/10.18186/thermal.1429072

[12] Madhuranthakam, C. M. R., & Sadeghian, R. (2024). Advances in Polyvinyl Alcohol-Based Membranes for Fuel Cells. Polymers, 16(13), 1775. https://doi.org/10.3390/polym16131775

[13] Liu, W., Chu, P. K., Feng, K., Shen, Y., Sun, H., D. Liu, Q. An, & X. Cai (2023). Performance of a proton exchange membrane fuel cell stack using conductive amorphous carbon-coated 304 stainless steel bipolar plates. Fuel Cells, 23(1), 1–10. https://doi.org/10.1016/J.JPOWSOUR.2010.05.019

[14] Mohanta, P. K., Thapa, R., & Sarmah, B. (2020) . Impact of membrane types and catalyst layers composition on performance of polymer electrolyte membrane fuel cells. Chemistry Open, 9(5), 607–615. https://doi.org/10.1002/open.202000089

[15] Mohanty, S., Nayak, A. K., & Sahu, S. (2021). Effects of the membrane thickness and ionomer volume fraction on the performance of PEMFC with U-shaped serpentine channel. International Journal of Hydrogen Energy, 46(39), 20650–20663. https://doi.org/10.1016/j.ijhydene.2021.03.252

[16] Okonkwo, P. C., Gbadegesin, A. S., & Bamgbade, A. O. (2021). Platinum degradation mechanisms in proton exchange membrane fuel cell (PEMFC) system: A review. International Journal of Hydrogen Energy, 46(29), 15850–15865. https://doi.org/10.1016/j.ijhydene.2021.02.078

[17] Ozdogan, M., Namlı, L., & Durmuş, A. (2019). Numerical investigation of effects of working conditions on performance of PEM fuel cell. Journal of Thermal Engineering, 5(1), 14–24. https://doi.org/10.18186/thermal.507919

[18] Sassin, B., Sassin, M. B., Uchaker, E., & Gerdes, K. (2016). Impact of compressive stress on MEA pore structure and its consequence on PEMFC performance. Journal of The Electrochemical Society, 163(8), F808–F815. http://dx.doi.org/10.1149/2.0291608jes

[19] Sassin, M. B., Sassin, B., Kreider, M., & McCreery, R. L. (2017). Fabrication method for laboratory-scale high-performance membrane electrode assemblies for fuel cells. Analytical Chemistry, 89(1), 511–518. https://doi.org/10.1021/acs.analchem.6b03005

[20] Schneider, P. D., Batool, M., Godoy, A. O., Singh, R., Gerteisen, D., Jankovic, J., & Zamel, N. (2023). Impact of platinum loading and layer thickness on cathode catalyst degradation in PEM fuel cells. Journal of The Electrochemical Society, 170(2), 024506. https://doi.org/10.1149/1945-7111/acb8df

[21] Sgarbi, R., Chatenet, M., Fabbri, E., Berchem, P., Flammenkamp, N., Hodnik, N., & Sauvage, F. (2023). Does the platinum-loading in proton-exchange membrane fuel cell cathodes influence the durability of the membrane-electrode assembly? Inorganic Chemistry Frontiers, 10(19), 7073-7084. https://doi.org/10.1039/D3IM00059A

[22] Shahgaldi, S., Alaefour, I., Li, M., & Wickramasinghe, S. (2018). Impact of ionomer in the catalyst layers on proton exchange membrane fuel cell performance under different reactant flows and pressures. Fuel, 227, 35–41. https://doi.org/10.1016/j.fuel.2018.04.076

[23] Shen, D., Wang, X., Li, Y., & Zhang, Z. (2018), Effect of MEA hot-pressing on the performance of direct methanol fuel cells. Proceedings of ICNMIM 2018, 402–404. http://dx.doi.org/10.26480/icnmim.01.2018.402.404

[24] Stähler, M., et al. (2019). A completely slot die coated membrane electrode assembly. International Journal of Hydrogen Energy, 44(14), 7053–7058. https://doi.org/10.1016/j.ijhydene.2005.05.012

[25] Solanki, A., & Pal, Y. (2021). A comprehensive review to study and implement solar energy in dairy industries. Journal of Thermal Engineering, 7, 1216–1238. https://doi.org/10.18186/thermal.978029

[26] Taner, T. (2019). A flow channel with Nafion membrane material design of PEM fuel cell. Journal of Thermal Engineering, 5(5),456–468. https://doi.org/10.18186/thermal.624085

[27] Thiyagarajan, P. K., Jeganathan, K., Panthalingal, M. K., & Rajappa, N. (2021). Effect of combinations of different operating parameters on performance of proton exchange membrane fuel cell. Thermal Science, 25(4A), 2731–2740. http://dx.doi.org/10.2298/TSCI201120070T

[28] Thiyagarajan, P. K., Jeganathan, K., & Panthalingal, M. K (2022). Combination studies of operating cell, inlet-line, and humidification temperatures on performance of proton exchange membrane fuel cell. Fuel Cells, 22(3),71–84. http://dx.doi.org/10.1002/fuce.202200022

[29] Wang, C., Zhang, Y., & Liu, J. (2019). Respective influence of ionomer content on local and bulk oxygen transport resistance in the catalyst layer of PEMFCs with low Pt loading. Journal of The Electrochemical Society, 166(4), F239–F245. http://dx.doi.org/10.1149/2.0401904jes

[30] Wang, X., Zhang, Y., Zhu, Y., Lv, S., Ni, H., Deng, Y., & Yuan, Y. (2022)0. Effect of different hot-pressing pressure and temperature on the performance of titanium mesh-based MEA for DMFC. Membranes (Basel),12(4),431. https://doi.org/10.3390/membranes12040431

[31] Xie, X., Zhang, G., Zhou, J., & Jiao, K. (2017). Experimental and theoretical analysis of ionomer/carbon ratio effect on PEM fuel cell cold start operation. International Journal of Hydrogen Energy, 42(17), 12521–12530. http://dx.doi.org/10.1016/j.ijhydene.2017.02.183

[32] Xing, L., Shi, W., Das, P. K., & Scott, K. (2017). Inhomogeneous distribution of platinum and ionomer in the porous cathode to maximize the performance of a PEM fuel cell. AIChE Journal, 63(11), 4895–4910. http://dx.doi.org/10.1002/aic.15826

[33] Xu, R., Deng, X., Zhang, E., Lei, J., & Liu, Y. (2024). Impact of nonuniform platinum loading distribution design in the catalyst layer on the high-temperature proton exchange membrane fuel cell performance. ACS Applied Energy Materials, 7(2), 427–437. https://doi.org/10.1021/acsaem.3c02260

[34] Yu, H., Roller, J. M., Mustain, W. E., & Maric, R. (2015). Influence of the ionomer/carbon ratio for low-Pt loading catalyst layer prepared by reactive spray deposition technology. Journal of Power Sources, 283, 84–94. https://doi.org/10.1016/j.jpowsour.2015.02.101

[35] Zhao, J., Liu, H., & Li, X. (2023). Structure, Property, and Performance of Catalyst Layers in Proton Exchange Membrane Fuel Cells. Electrochemical Energy Reviews, 6, 13. https://doi.org/10.1007/s41918-022-00175-1

[36] Zhou, Z.-Q., Wang, J.-X., Hu, H.-Y., & Hou, H.-L. (2025). Achievements in protective coatings for metallic bipolar plates in proton exchange membrane fuel cells: A comprehensive review. Engineering Research Express, 7(2), 022001. https://doi.org/10.1088/2631-8695/adc34c